Author Manuscript

Author Manuscript

Author Manuscript

Author Manuscript

HHS Public Access

Author manuscript

J Neurosci Methods. Author manuscript; available in PMC 2018 January 02.

Published in final edited form as:

J Neurosci Methods. 2018 January 01; 293: 86–96. doi:10.1016/j.jneumeth.2017.09.010.

Temporal remodeling of pial collaterals and functional deficits in a murine model of ischemic stroke

Benjamin Okyere, **Miranda Creasey**, **Yeonwoo Lebovitz**, and **Michelle H. Theus***

The Department of Biomedical Sciences and Pathobiology, Virginia-Maryland Regional College of Veterinary Medicine, 970 Washington St. SW, Blacksburg, VA, 24061, USA

Abstract

Background—Leptomeningeal anastomoses play a critical role in regulating reperfusion following cerebrovascular obstruction; however, methods to evaluate their temporospatial remodeling remains under investigation.

New method—We combined arteriole-specific vessel painting with histological evaluation to assess the density and diameter of inter-collateral vessels between the middle cerebral artery and anterior cerebral artery (MCA-ACA) or posterior cerebral artery (MCA-PCA) in a murine model of permanent middle cerebral artery occlusion (pMCAO).

Results—While the overall density was not influenced by pMCAO, the size of MCA-ACA and MCA-PCA vessels had significantly increased 2 days post-pMCAO and peaked by 4 days compared to the un-injured hemisphere. Using a combination of vessel painting and immunofluorescence, we uniquely observed an induction of cellular division and a remodeling of the smooth muscle cells within the collateral niche following post-pMCAO on whole mount tissue sections. Vessel painting was also applied to pMCAO-injured Cx3cr1^{GFP} mice, in order to identify the spatial relationship between Cx3cr1-positive peripheral-derived monocyte/macrophages and the vessel painted collaterals. Our histological findings were supplemented with analysis of cerebral blood flow using laser Doppler imaging and behavioral changes following pMCAO.

Comparison with existing methods—Compared to polyurethane and latex methods for collateral labeling, this new method provides detailed cell-type specific analysis within the collateral niche at the microscopic level, which has previously been unavailable.

Conclusions—This simple and reproducible combination of techniques is the first to dissect the temporospatial remodeling of pial collateral arterioles. The method will advance investigations into the underlying mechanisms governing the intricate processes of arteriogenesis.

Keywords

pMCAO; Pial collateral vessels; Cerebral blood flow; Smooth muscle cell; Vascular remodeling and arteriogenesis

*Corresponding author at: Department of Biomedical Sciences and Pathobiology, Virginia-Maryland Regional College of Veterinary Medicine, Virginia Tech, 970 Washington St. SW (0910), Blacksburg, VA 24061, USA. mtheus@vt.edu (M.H. Theus).

Author Manuscript Author Manuscript Author Manuscript Author Manuscript

1. Introduction

Leptomeningeal anastomoses or pial collateral vessels are arteriole-to-arteriole connections joining the major branches of the cerebral arteries (middle MCA, anterior ACA and posterior PCA) in the pial surface of the brain. These specialized bypass vessels, which are normally inactive, are capable of re-routing blood flow around vascular obstruction (van Royen et al., 2001; Toriumi et al., 2009; Shuaib et al., 2011). Although patients having greater collateral vessel density show improved recanalization and reduced infarct size following MCA occlusion, substantial variation in size, number and compensatory capacity of collaterals exist (Zhang et al., 2016). The pial collateral network forms during prenatal development, although secondary changes related to various pathophysiological conditions may occur throughout life (Liebeskind 2003; Chalothorn and Faber, 2010a, 2010b). Vascular endothelial growth factor (VEGF), A Disintegrin and Metalloproteases (ADAM) 10 and 17, chloride intracellular channel (Clic4) and Eph receptor tyrosine kinase EphA4 have been shown to regulate murine collateral density and diameter during perinatal development as well as remodeling after ischemia (Chalothorn et al., 2007; Clayton et al., 2008; Chalothorn et al., 2009; Lucitti et al., 2012; Okyere et al., 2016). Collateral vessel remodeling, also known as arteriogenesis, results in their enlargement or outward growth which enables restoration of retrograde re-perfusion into the territory of the occluded vessel (Takahashi, 1980; Takahashi et al., 1980; Drake et al., 1994; Yamada et al., 1996; Iwama et al., 1998; Lownie et al., 2000; Brozici et al., 2003).

Arteriogenesis occurs in three phases: initiation, growth and maturation (Meisner and Price, 2010). Initiation of collateral remodeling occurs when collateral blood flow, which normally moves in both directions but in equilibrium, becomes disrupted leading to increased unidirectional flow within the collateral vessel. This steep pressure gradient causes fluid shear stress to activate the endothelium, invoking a cascade of events (Buschmann et al., 2003; Heil et al., 2006; Toriumi et al., 2009) that leads to the production of cytokines, growth factors and proteases which mediate the enlargement of the collateral vessels (Heil et al., 2002; Schaper and Scholz, 2003; Cai and Schaper, 2008; Li et al., 2016). Enhancement of retrograde cerebral blood flow through remodeled collateral vessels into the territory of the occluded artery mitigates cellular damage and helps maintain tissue preservation (Crisostomo et al., 1993; Beretta et al., 2015; Liu et al., 2015; Winship, 2015; Cuccione et al., 2016; van Seeters et al., 2016; Beretta et al., 2017). Thus, enhancing collateral growth and remodeling has become an attractive target for therapeutic intervention in patients suffering from an ischemic attack (Schierling et al., 2011; Chen et al., 2014; Nishijima et al., 2015). However, the cellular and molecular cues regulating this response remains under investigation.

To investigate the dynamic changes occurring in the collateral network, *in vivo* imaging and histological analysis are often used. *In vivo* imaging techniques, such as optical coherence tomography, two-photon microscopy and laser speckle imaging have been used to observe collateral reperfusion and remodeling in pathological states (Schaffer et al., 2006; Defazio et al., 2011; Defazio et al., 2012; Li et al., 2016). Such methods are particularly useful for non-invasive, longitudinal assessment of collateral function with high resolution. However, to improve our understanding of the cellular and molecular mechanism(s) underlying these

Author Manuscript Author Manuscript Author Manuscript Author Manuscript

processes we have developed a histological method combining vessel painting and immunocytochemistry using cortical whole mounts for quantitative and qualitative analysis of the structural changes within and around the wall of the collateral itself. This method will provide detailed cell-type specific analysis of the collateral niche at the microscopic level, which has previously been unavailable. Knowledge gained from such findings will expand our understanding of the individual cell response within and surrounding the collateral during active remodeling, including endothelial, smooth muscle and immune-derived cell morphology changes.

Few studies have evaluated the histological and morphological features of collateral remodeling. Coyle and colleagues developed the use of latex perfusion and casting of the cerebral-vasculature (Coyle and Jokelainen, 1982; Coyle and Heistad, 1991). This technique, however, labels both the venal and arterial vascular system. The use of polyurethane to characterize the pial collaterals has also been described (Zhang et al., 2010). While both techniques provide superior visualization of collaterals, they cannot be combined with immunofluorescence labeling. Our method provides detailed morphological and histological changes occurring in the pial collateral network, after surgically inducing stroke in the brain, and selectively labeling the arterial vasculature using a vessel painting technique. Using a combination of methods, our findings illustrate the stepwise changes in collateral growth following (Defazio et al., 2011; Okyere et al., 2016) and quantify changes occurring in individual dorsal pial collateral vessels including cell proliferation, smooth muscle cell reorganization and recruitment of Cx3cr1GFP-expressing peripheral-derived immune cells (Defazio et al., 2011; Okyere et al., 2016). We also describe the longitudinal relationship between these structural alterations and cerebral blood flow as well as behavioral deficiencies in the pMCAO model. These findings provide a standardized platform for evaluating the molecular and cellular mechanism(s) underlying collateral remodeling which may aid therapeutic interventions to enhance this adaptive response and improve acute neural functional outcome following stroke.

2. Materials and methods

2.1. Animals

All mice were generated and housed in an AAALAC approved, virus/antigen-free facility with a 12 h light-dark cycle; food and water *ad libitum*. CD1 mice were purchased from Charles Rivers, and bred until desired numbers were generated for experimentation. All experiments were conducted in accordance with the NIH Guide for the Care and Use of Laboratory Animals and were conducted under the approval of the Virginia Tech Institutional Animal Care and Use Committee (IACUC; #15-063) and the Virginia Maryland Regional College of Veterinary Medicine. All efforts were made to minimize the number of animals used and their suffering.

2.2. Surgical procedure

Focal ischemic stroke was induced by pMCAO as previously referenced with slight modifications (Colak et al., 2011). Briefly, 8–12 week-old mice (25–35 g) were injected with analgesic Buprenorphine-SR (0.15 mg/kg), and anesthesia induced with 2%

Author Manuscript Author Manuscript Author Manuscript Author Manuscript

isoflurane-30% oxygen mixture. Body temperature was monitored with a rectal probe and maintained at 37 °C with a controlled heating pad (homeothermic blanket system; Harvard Apparatus). Subsequently, the skull was thinned, at the junction of zygomatic arch and squamosal bone, to expose the MCA. The main branch of the MCA, and two adjacent branches were ligated using a small vessel cauterizer. Sham controls received the same surgical procedures without ligation of the MCA. Following injury, the incision was closed using Vetbond tissue adhesive (3 M, St. Paul, MN, USA) and animals were returned to their home cage on a heating pad for post-op monitoring.

2.3. Vessel painting

Vessel painting on adult CD1 mice was performed as previously described (Defazio et al., 2011; Okyere et al., 2016). Briefly, mice were injected with heparin (2000 units/kg), and sodium nitroprus-side (SNP, 0.75 mg/kg) five minutes prior to euthanization, using an overdose of isoflurane. When breathing stopped, the chest cavity was opened and then cardiac perfused using a Gilson MiniPuls3 peristaltic perfusion pump (Gilson Scientific, Bedfordshire, UK). Using a continuous infusion, 10 ml of 1X phosphate buffered saline (1X PBS) containing 20 units/ml heparin was perfused to flush blood from the circulatory system, then 10 ml DiI (0.01 mg/ml, Invitrogen) diluted in 4% sucrose–PBS-heparin mixture was perfused using a flow rate of 2 ml/min followed by cold 4% paraformaldehyde (PFA) to fix the tissue. After perfusion, brains were carefully removed from the skull and placed in PFA overnight. Fixed brains were imaged at high resolution using multiple image planes at 4× magnification on an upright fluorescence microscope (BX-51, Olympus America), using mosaic tile imaging from StereoInvestigator software (MBF, Williston, VT). Scaled mosaic images were imported into ImageJ (NIH), then the total numbers of intra- and inter-tree collaterals were identified between and within the MCA, ACA, and PCA artery branches and quantified using the counting tool in ImageJ on each mosaic image. Pial collateral diameters were also individually assessed on the scaled mosaic images using ImageJ by averaging three independent diameters along the collateral length. Diameters of individual collaterals were also confirmed using 20× magnification and the line measure tool on MBF StereoInvestigator software at three locations along the length of the collateral. Collateral length and span were also measured to determine collateral tortuosity. Length was measure with the straight line tool by drawing a straight line from the start to the end point of the collateral. Span was measured with the freehand line tool by tracing the collateral from the start to end point. Tortuosity index was calculated as a ratio of the length:span of each collateral.

2.4. Immunostaining cortical whole mounts

For immunostaining, the surface cortical region of the brain was dissected and placed in 1X PBS overnight in preparation for whole mount staining. Whole mounts were subsequently blocked in 2% Fish gelatin (Sigma Aldrich, St. Louis, MO) with 0.1% Triton X-100 for 3 h then incubated overnight in antibodies against smooth muscle actin (SMA) (1:1000; Abcam, Cambridge, UK; ab7817) in blocking buffer at 4 °C. Whole mounts were washed 5 times with 1X PBS then incubated with anti-mouse Alexa Fluor 488 conjugated secondary antibody (Molecular Probes, Carlsbad, CA) overnight at 4 °C. After washing 5× with 1X PBS, whole mounts were counterstained with DAPI (ThermoFisher Scientific, Waltham,

Author Manuscript Author Manuscript Author Manuscript Author Manuscript

MA) for 5 min, washed 3× with 1X PBS and embedded in mounting media (SouthernBiotech, Birmingham, AL) in a 35 mm glass dish, cover slipped, then imaged on an inverted Zeiss 880 confocal microscope (Carl-Zeiss, Oberkochen, Germany). For PCNA staining, whole mounts were incubated in HCL for 45 min at 37 °C and then neutralized with sodium borate as previously described (Kennedy et al., 2000). This method is used to unmask the PCNA antigen. Tissue was blocked then incubated in rabbit anti-PCNA antibody (1:1000; Cell signaling, Danvers, MA) overnight, and then incubated with anti-rabbit 488 (Invitrogen, Carlsbad, CA) secondary antibody. The contralateral hemisphere was used as a negative control.

2.5. Behavioral testing

2.5.1. Rotarod—We used the Rotarod (Rotamex, Columbus Inst) to assess motor function as previously reported (Jones and Roberts, 1968; Bouet et al., 2007). Briefly, animals were pre-trained for 4 consecutive days prior to pMCAO or sham injury. The starting velocity was set at 10 rpm and accelerated to 0.1 rpm/sec. A baseline was collected on the fourth day, then again at 3, 7, 14, 28, and 35 days post-pMCAO or sham injury for each mouse. Data is graphed as the mean of the individual scores relative to baseline.

2.5.2. Grip test—A rodent grip strength meter (DFIS 10, Columbus Instruments, Columbus, OH) was used to measure strength in the forelimbs. Mice were first allowed to grasp the apparatus bar, then pulled perpendicular to the bar. Grip strength was recorded in Newtons (N) at baseline (one day prior to injury) then at 3, 7, 14, 28, and 35 days post-pMCAO or sham injury. Data is represented as relative to baseline.

2.5.3. Inverted screen or grip test—We used the Kondziela inverted screen test to assess muscle strength after injury (Deacon, 2013). The inverted screen contained a 43 cm^2 wire mesh consisting of 12 mm squares of 1 mm diameter wire. Mice were pre-trained, for 4 consecutive days, to grip the screen as it is inverted and a baseline time to fall was recorded on the last day of training then again at 3, 7, 14, 28, and 35 days post-pMCAO or sham injury.

2.5.4. Beam walk—The beam walk test was used to assess fine motor coordination and balance. The beam was 30 cm in height, 6 mm in diameter and 80 cm long. Mice were pre-trained and the time to traverse the beam was recorded on the last day of training and at 3–35 post-injury.

2.5.5. Neurological severity scoring (NSS)—The NSS was used to assess sensorimotor deficits pre-injury and at 3–35 days post-injury. NSS is a composite of motor, sensory (visual, tactile and proprioceptive), reflex, and balance tests. Function was graded on a scale of 0–14 (normal = 0; maximal deficit = 14), where 1 point is awarded for the inability to perform the task or for the absence of the tested activity as previously described (Theus et al., 2008).

2.5.6. Novel object recognition (NOR)—Cognitive and spatial deficits were tested using the novel object recognition task. Briefly, mice were introduced to two identical

Author Manuscript Author Manuscript Author Manuscript Author Manuscript

objects on day one and then one of the objects was replaced with a new object the following day (test day) in a 40 cm^3 arena. Time of exploration of the old and new object was recorded over 5 min. Preference of object was calculated as a ratio exploration time of the specific object to the total time of exploration of both objects. NOR was also administered at 3–35 days post-injury.

2.6. Cerebral blood flow

Cerebral blood flow (CBF) was assessed at pre-, 5 min and 1–4 day post-injury using the Moor LDI2-HIR Laser Doppler flowmeter with Moor Software Version 5.3 (Moor Instruments, Wilmington, DE). Briefly, mice were anesthetized with 1.25% isoflurane-O_2, the skin opened to expose the scalp transversely, and head placed in a stereotactic device. Rectal temperature was maintained at 37.0 ± 0.5 °C and cerebral blood flow, in perfusion units (PFU) was scanned using a 2.5 cm × 2.5 cm scanning area. Tissue perfusion was quantified with a region of interest (ROI) define in the same left hemisphere of injury and represented a ratio of post-perfusion units (PFU) relative to the pre-injury scan of each mouse.

2.7. Statistical analysis

Data was graphed using GraphPad Prism, version 4 (GraphPad Software, Inc., San Diego, CA). Student's two-tailed *t*-test was used for comparison of two experimental groups. Multiple comparisons were done using one-way or two-way ANOVA where appropriate followed by *post hoc* Bonferroni test. Changes were identified as significant at P value <0.05. Mean values were reported together with the standard error of mean (SEM).

3. Results

3.1. Murine permanent middle cerebral artery occlusion (pMCAO) model and cerebral blood flow

Collateral density and remodeling plays a critical role in restoring cerebral blood flow after arterial occlusion (Coyle and Heistad, 1991). First we evaluated the time course of reperfusion to the ipsilateral cortex following pMCAO, by assessing cerebral blood flow (CBF) using high resolution Laser Doppler imaging (moorLDI2-HIR). Laser Doppler images revealed distinct difference in ipsilateral CBF between sham operated and pMCAO mice immediately after injury (Fig. 1A vs B; respectively). Statistical analysis correlated with reperfusion images. CBF was represented by quantifying the perfusion units (PFU) relative to pre-injury scan values (Fig. 1C). Immediately after pMCAO, CBF is significantly reduced (0.42 ± 0.03 PFU) in the ipsilateral hemisphere compared to pre-injury levels (0.99 ± 0.02 PFU). However, perfusion values are increased at day 1 (0.65 ± 0.01 PFU), day 2 (0.73 ± 0.03), day 3 (0.75 ± 0.03 PFU) and day 4 (0.77 ± 0.03 PFU) compared to 5 min post-pMCAO. A significant increase (16%) in CBF was observed between 1d and 4d post-pMCAO. These findings demonstrate a 57% reduction in CBF following pMCAO in CD1 mice, which is restored to 65% of the pre-injury levels by 1 day and 80% by 4 days post-pMCAO. TTC staining of coronal brain slices confirms a focal area of cortical tissue loss in the left hemisphere (Fig. 1E) compared to sham-injured control (Fig. 1D) as a result of these changes in CBF.

Author Manuscript Author Manuscript Author Manuscript Author Manuscript

3.2. Collateral remodeling after pMCAO

The MCA is one of the major arteries that provides blood supply to the brain and connects to the anterior and the posterior cerebral arteries via the MCA-ACA and MCA-PCA collateral networks, respectively. Following pMCAO, the outward growth and remodeling of pial collateral vessels provides an alternative route for retrograde reperfusion into the MCA territory. To correlate changes in CBF after pMCAO with collateral density and remodeling, we used vessel painting to label the adult arterial network, as previously demonstrated (Okyere et al., 2016), and assessed the pial collateral remodeling at 1, 2, 4, 7, and 65 days post-pMCAO on the ipsilateral and contralateral hemispheres. Collateral diameter and tortuosity was assessed as parameters of collateral remodeling at each time point. The overall collateral diameter was significantly increased in the ipsilateral cortex at 2d (34 ± 2 μm vs 20 ± 1 μm), 4d (39 ± 3 vs 20 ± 1 μm), 7d (38 ± 1 μm vs 20 ± 1 μm) and 65d (40 ± 2 μm vs 20 ± 1 μm) post-pMCAO compared to contralateral. No significant change was observed at 1 day (24 ± 2 μm vs 19 ± 1 μm) (Fig. 3A). Similarly, we found a significant increase in collateral size between both MCA-ACA (Fig. 3B) and MCA-PCA (Fig. 3C) indicating both MCA-ACA and MCA-PCA collaterals enlarge in response to pMCAO. We then analyzed the percentage of pial collaterals at 10–20 μm, 21–30 μm, 31–40 μm, <40 μm in the contralateral and ipsilateral hemisphere at 1–65d post-pMCAO (Fig. 2D). Approximately ninety-percent of un-injured collaterals were 10–30 μm in size, which reduced to ~70% at 1d, ~40% at 2d, and ~30% at 4, 7 and 65d in the ipsilateral cortex after pMCAO. A concomitant increase in the percentage of >40 μm collaterals at 1d (8.40 ± 0.07%), 2d (27.59 ± 5.19%), 4d (56.30 ± 5.23%), 7d (56.09 ± 5.44%) and 65d (45.73 ± 9.83%). No significant differences were seen in inter-collateral counts (MCA-ACA and MCA-PCA) or total collateral counts (inter- and intra-collaterals) between ipsilateral and contralateral sides (Fig. 2E and F; respectively). We observed an increased trend in the average tortuosity index (TI) between 1d (1.13 ± 0.01 TI) and 4d (1.22 ± 0.02 TI) in the ipsilateral compared to contralateral collaterals, although its difference was non-significant. These data indicate that a majority of the collateral growth in size occurs between 1 and 4 days in CD1 mice, an effect maintained up to 65 days post-pMCAO.

3.3. Histological evaluation of collateral remodeling after pMCAO

The acute temporal remodeling of pial collaterals in CD1 mice can be characterized after pMCAO using vessel painting (Okyere et al., 2016) and standard histological evaluation of cortical whole mounts. We determined that vessel painting can be used in combination with antibodies against smooth muscle actin (SMA) to qualitatively assess the dynamic changes in vessel shape and smooth muscle cell (SMC) location as well as quantify cellular processes, such as proliferation, during collateral remodeling. Following vessel painting (VP) with the lipophilic and fluorescent Dil at 1, 2 and 4 days post-injury, perfused whole mount tissues were stained with anti-SMA and imaged using confocal microscopy to visualize smooth muscle cell reorganization during arteriogenesis, a key step in collateral remodeling (Scholz et al., 2000; Meisner and Price 2010). Visible changes in the size of pial collaterals are seen following pMCAO and 4 days post-pMCAO compared to sham injury (Fig. 3A–D). The number of collaterals undergoing remodeling is also increased during this time (Fig. 3B–D; white arrows). Whole mounts stained with anti-SMA and imaged using confocal microscopy show reduced staining and significant re-organization of smooth

Author Manuscript Author Manuscript Author Manuscript Author Manuscript

muscle cells in collateral vessels at 4d post-pMCAO (Fig. 3C–E and C1–E1) compared to 7d day post-pMCAO (Fig. 3F–H) where increased SMA coverage is seen and coverage of the vessel is underway. During this time it is known that SMCs exit the vessel wall, expand and reengage once the vessel has grown to full capacity. These findings demonstrate a useful histological tool for evaluating SMC changes on vessel painted pial collaterals as a means to delineate dynamic temporospatial structural features of remodeling vessels during arteriogenesis (Chalothorn and Faber, 2010a, 2010b).

3.4. Collateral remodeling in Cx3cr1^{GFP} mice after pMCAO

The contribution of peripheral-derived immune cells during collateral remodeling has recently been demonstrated (la Sala et al., 2012; Troidl et al., 2013). For example, pharmacological monocyte depletion and athymic nude mice that lack T cells display impaired arteriogenesis (Couffinhal et al., 1999; Heil et al., 2002). CD4- and CD8-deficient mice also show reduced collateral circulation and are thought to be mediators of collateral recruitment (Stabile et al., 2003; Stabile et al., 2006). To test whether we could visualize with high resolution the recruitment of immune-derived cells to the peri-vascular region of remodeling collaterals on vessel painted whole mounts, we used genetic Cx3cr1^{GFP} knock-in reporter mice. Cx3 chemokine receptor 1 (Cx3cr1) is expressed by monocytes, macrophages, subsets of NK and dendritic cells and brain microglia (Jung et al., 2000). At 4 days post-pMCAO, using confocal image analysis, we observed a significant recruitment of GFP-positive cells on and around the remodeling collateral vessels in the ipsilateral hemisphere (Fig. 4A1–A3) compared to contralateral (Fig. 4B–D). Higher magnification of a collateral vessel undergoing remodeling (identified as vessels at or greater than 30 μm in the ipsilateral hemisphere) clearly shows the peri-vascular nature of the immune-derived GFP-positive cells (Fig. 4E–G; 4E ortho view showing non-overlap of GFP and the vessel painted arteriole, compared to the underlying ramified microglia in the brain parenchyma (Fig. 4A) of the whole mounts. To our knowledge, this is the first high resolution demonstration of Cx3cr1^{GFP} –positive cell recruitment to the pial collaterals undergoing remodeling following ischemic stroke. Because these cells are snathey likely represent peripheral-derived immune cells and not brain parenchymal microglia. Additional co-labeling using this technique could also be employed to specifically identify and quantify the Cx3cr1^{GFP} expressing cells during the remodeling phases.

3.5. Cell proliferation in the collateral niche

Endothelial and smooth muscle cell proliferation is a key step in the arteriogenic process. Several biological markers such as BrdU (5-Bromo-2′-deoxyuridine) and EdU (5-ethynyl-2′-deoxyuridine) can be used to identify proliferating cells during remodeling, but they can be expensive and only label a snapshot of cells in the s-phase of the cell cycle. In order to identify all cells undergoing cellular proliferation we used antibodies against proliferating cell nuclear antigen (PCNA), which is expressed in the nucleus of dividing cells and is a cofactor of DNA polymerase delta (Flores-Rozas et al., 1994; Imura et al., 2004). In addition to the recruitment of peripheral-derived immune cells to the arteriogenic region, numerous PCNA-positive cells are seen on and around growing collaterals in the ipsilateral hemisphere (Fig. 5B) compared to contralateral (Fig. 5A) following pMCAO. High magnification confocal imaging demonstrates numerous PCNA-positive cells within the VP-

Author Manuscript Author Manuscript Author Manuscript Author Manuscript

stained vessel wall (Fig. 5C–E). These findings highlight the unique cellular changes that occur during active remodeling using vessel painting and histological examination in a murine model of ischemic stroke.

3.6. Comprehensive behavioral assessment after pMCAO

In order to determine whether the time course of behavioral deficits correlates with that of collateral remodeling we administered a comprehensive battery of behavioral tasks after ischemic stroke. Sensorimotor deficits have not been previously described for this model. We assessed sensory and balance coherence by using a 14-point neurological severity scoring system, which tests motor, sensory and reflex activity. Injured mice had consistent deficits in head axis placement, balancing, proprioception in forelimbs and occasionally in their hind limbs, as well as corneal and startle reflexes. Neurological severity scores were significantly increased at each time point compared to sham injury (Fig. 6A). Motor activity was also determined by several tasks. Rotarod performance showed that mice develop severe motor deficits after pMCAO (Fig. 6B). Further motor functional assessment using the beam walk test (Fig. 6D) and grip test (Fig. 6F) confirmed the motor deficits in the pMCAO model. Moreover, we tested murine strength after injury using the inverted screen and grip strength tests. Although the inverted screen test did not yield consistent significant differences in performances between sham and pMCAO-injured mice (Fig. 6E), the grip meter test for forelimb strength displayed consistent deficits (Fig. 6F) at 3, 7, 14 and 28 days. Finally, the use of the novel object recognition test, a simple assay of memory and novelty preference that relies on a rodent's innate exploratory behavior (Antunes and Biala, 2012), was evaluated following pMCAO or sham injury. As early as 3 days post-injury, pMCAO mice had deficits in their memory function which persisted up to 35 days compared to sham (Fig. 6C). These data show that focal cerebral ischemia induces long-lasting sensorimotor, as well as learning and memory deficits following pMCAO. Since no further growth of collateral vessels occurs after 4 days post-pMCAO, the sustained behavioral impairments from 3 to 35 days post-pMCAO may be affected by early collateral remodeling.

4. Discussion

Targeting the adaptive response of the collateral circulation is an emerging strategy for effective therapy against ischemic stroke, where several pre-clinical studies show enhancement of arterio-genesis greatly affects the severity of neural injury (Jung et al., 2013; Liebeskind et al., 2014). However, the mechanisms underlying collateral remodeling remain under investigation. The current study aimed to catalog changes in the murine pial collateral network in a pMCAO stroke model (Llovera et al., 2014) using a novel method that combines histological detection for cell-type specific changes on vessel painted collaterals. Analysis of collateral remodeling was complemented with histological analyses to show the versatility of the technique. Finally, CBF restoration and behavioral outcomes that occur following pMCAO were assessed to develop a platform for quantifying functional recovery in parallel with collateral analysis, which have not previously been demonstrated for this model.

Author Manuscript Author Manuscript Author Manuscript Author Manuscript

Collateral circulation and injury-induced remodeling have been assessed by standard angiographic techniques, including digital subtraction angiography, computed tomography and magnetic resonance (MR) angiography, as well as a growing array of advanced MR techniques including arterial spin labeling and dynamic MR angiography (Raymond and Schaefer, 2017), as well as other *in vivo* methods. Recently, studies have utilized latex, polyurethane-filled arteriograms, or genetically modified mice, ephrinB3^{lacz}, to label and analyze collateral remodeling (Coyle and Jokelainen, 1982; Coyle and Heistad, 1991; Chalothorn and Faber, 2010a, 2010b). The current study evaluated the ease of use and the histological flexibility of vessel painting to identify and evaluate the remodeling of pial collaterals after pMCAO. When whole mount cortical tissue preps following vessel painting are assessed using confocal image analysis, detailed information at the cellular level can be provided at high resolution. This includes temporospatial determination of cell-to-cell interactions (SMC, immune cells and vessel painted ECs), cell dynamics (proliferation and survival) and regional distribution of the remodeling process along the length of the collateral vessel. Although not emphasized in the results, we found ‘hot spot’ areas of remodeling on the growing collaterals. The significance of these findings, underlying mechanism(s) and evaluation across different species such as mouse, rat and swine are currently underway. Moreover, this technique has been successfully used in other models of brain injury in our laboratory, including controlled cortical impact and repeated mild traumatic brain injury. The current study shows that the active remodeling of pial collaterals occurs predominantly between day 1 and 4 post-pMCAO. Similar results of collateral remodeling have been reported elsewhere using different murine strains of mice (Zhang et al., 2010). Both MCA-ACA and MCA-PCA collaterals increased in size at a similar rate in the ipsilateral hemispheres compared to the un-injured contralateral hemisphere. Furthermore, the peak of collateral enlargement correlates with the greatest improvement in CBF. These findings suggest retrograde reperfusion may occur via the ACA as well as PCA following MCA occlusion.

Few studies have analyzed the temporal dynamic changes in SMCs on pial collaterals during arteriogenesis. Confocal microscopy revealed distinct temporal changes in expression of SMA during arteriogenesis. As early as day 4 post-pMCAO, ipsilateral collaterals undergoing remodeling showed reduced expression of SMA compared to contralateral collaterals. Interestingly, we observed numerous expanding or bulging sites on collaterals undergoing remodeling, which coincided with a reduction in SMA expression and a change in location and organization of SMCs. The inverse correlation between the increasing size and SMA expression suggests SMC reorganization is necessary for the outward growth and remodeling. These temporal expressional changes have been suggested to be required for the infiltration of peripheral-derived immune cells during luminal expansion of the collateral vessel (Wolf et al., 1998; Scholz et al., 2000). Owing to an increase in unidirectional flow through the collateral vessel, shear stress activates mechanoreceptors on endothelial cells (ECs) to initiate the production of key signals that influence the surrounding cells, resulting in the adaptive outward growth response in including EC and SMC division (van Royen et al., 2001; Schaper and Scholz, 2003; Heil et al., 2006; Cai and Schaper, 2008). Indeed, the PCNA-positive cells located within and surrounding the collateral wall in the ipsilateral hemisphere after pMCAO likely represents actively dividing SMCs and ECs, as well as

Author Manuscript Author Manuscript Author Manuscript Author Manuscript

infiltrating monocytes/macrophages. The versatility of vessel painting can allow for further assessment of the location and identity of PCNA-positive cells.

Finally, a battery of sensorimotor behavioral tests were performed to assess reliable modes of analyzing neurological deficits after stroke. A longitudinal behavioral assessment was administered to experimental mice to gauge neurological deficits in our model. The hippocampus plays an important role in the spatial memory in animals (Olton et al., 1978; Squire, 1992; Squire et al., 1992). Although the MCA does not directly supply blood to the hippocampus, it has been postulated that cognitive deficits may be due to hippocampal denervation from the infarcted cortex, thalamic atrophy, or denervated basal nucleus cholinergic fibers to the cortex, as well as neocortical sites within the MCA region (Fujie et al., 1990; Kataoka et al., 1991). Numerous behavioral analyses have been used to assess cognitive deficits including the Morris water maze (MWM) and the novel object recognition (NOR) tests. However, investigation of deficits in spatial memory using the MWM may be confounded by coexisting sensory and motor impairments (Bingham et al., 2012). Thus, learning and memory were evaluated using NOR because it is sensitive to hippocampal function (Broadbent et al., 2010). Ischemic-injured mice showed NOR deficit up to 65 days post. In addition, a comprehensive neurological severity test was used to assess sensorimotor function. The NSS constitutes motor, sensory, and reflex activities. Our studies showed significant and clear deficits in pMCAO-injured mice compared to shams. Finally, because the injury also involves the primary motor cortex, we performed the Rotarod, beam balance, screen inversion and grip strength tests in order to gauge motor and muscular strength deficits. These studies have been performed in a rat model of MCAO and were modified for mice (Theus et al., 2008). These current findings provide a standardized platform for evaluating the molecular mechanism(s) controlling collateral remodeling in order to develop novel strategies aimed at enhancing this adaptive response and improving neural functional outcome following stroke.

Acknowledgments

This work was supported by the National Institute of Neurological Disorders and Stroke of the National Institutes of Health under Award Number F31NS095719 (BO), R01NS096281 (MHT), R15 NS081623 (MHT) and R25 GM0727-09 (IMSD). The content is solely the responsibility of the authors and does not necessarily represent the official views of the National Institutes of Health. We recognize the VT-IMSD Programs for student support (BO) and the Virginia-Maryland Regional College of Veterinary Medicine.

References

Antunes M, Biala G. The novel object recognition memory: neurobiology, test procedure, and its modifications. Cogn Process. 2012; 13(2):93–110. [PubMed: 22160349]

Beretta S, Cuccione E, Versace A, Carone D, Riva M, Padovano G, Dell'Era V, Cai R, Monza L, Presotto L, Rousseau D, Chauveau F, Paterno G, Pappada GB, Giussani C, Sganzerla EP, Ferrarese C. Cerebral collateral flow defines topography and evolution of molecular penumbra in experimental ischemic stroke. Neurobiol Dis. 2015; 74:305–313. [PubMed: 25484287]

Beretta S, Versace A, Carone D, Riva M, Dell'Era V, Cuccione E, Cai R, Monza L, Pirovano S, Padovano G, Stiro F, Presotto L, Paterno G, Rossi E, Giussani C, Sganzerla EP, Ferrarese C. Cerebral collateral therapeutics in acute ischemic stroke: a randomized preclinical trial of four modulation strategies. J Cereb Blood Flow Metab. 2017 271678X16688705.

Author Manuscript Author Manuscript Author Manuscript Author Manuscript

Bingham D, Martin SJ, Macrae IM, Carswell HV. Watermaze performance after middle cerebral artery occlusion in the rat: the role of sensorimotor versus memory impairments. J Cereb Blood Flow Metab. 2012; 32(6):989–999. [PubMed: 22373646]

Bouet V, Freret T, Toutain J, Divoux D, Boulouard M, Schumann-Bard P. Sensorimotor and cognitive deficits after transient middle cerebral artery occlusion in the mouse. Exp Neurol. 2007; 203(2): 555–567. [PubMed: 17067578]

Broadbent NJ, Gaskin S, Squire LR, Clark RE. Object recognition memory and the rodent hippocampus. Learn Mem. 2010; 17(1):5–11. [PubMed: 20028732]

Brozici M, van der Zwan A, Hillen B. Anatomy and functionality of leptomeningeal anastomoses: a review. Stroke. 2003; 34(11):2750–2762. [PubMed: 14576375]

Buschmann I, Katzer E, Bode C. Arteriogenesis – is this terminology necessary? Basic Res Cardiol. 2003; 98(1):1–5. [PubMed: 12494262]

Cai W, Schaper W. Mechanisms of arteriogenesis. Acta Biochim Biophys Sin (Shanghai). 2008; 40(8): 681–692. [PubMed: 18685784]

Chalothorn D, Faber JE. Formation and maturation of the native cerebral collateral circulation. J Mol Cell Cardiol. 2010a; 49(2):251–259. [PubMed: 20346953]

Chalothorn D, Faber JE. Strain-dependent variation in collateral circulatory function in mouse hindlimb. Physiol Genomics. 2010b; 42(3):469–479. [PubMed: 20551146]

Chalothorn D, Clayton JA, Zhang H, Pomp D, Faber JE. Collateral density, remodeling, and VEGF-A expression differ widely between mouse strains. Physiol Genomics. 2007; 30(2):179–191. [PubMed: 17426116]

Chalothorn D, Zhang H, Smith JE, Edwards JC, Faber JE. Chloride intracellular channel-4 is a determinant of native collateral formation in skeletal muscle and brain. Circ Res. 2009; 105(1):89–98. [PubMed: 19478202]

Chen J, Venkat P, Zacharek A, Chopp M. Neurorestorative therapy for stroke. Front Hum Neurosci. 2014; 8:382. [PubMed: 25018718]

Clayton JA, Chalothorn D, Faber JE. Vascular endothelial growth factor-A specifies formation of native collaterals and regulates collateral growth in ischemia. Circ Res. 2008; 103(9):1027–1036. [PubMed: 18802023]

Colak G, Filiano AJ, Johnson GV. The application of permanent middle cerebral artery ligation in the mouse. J Vis Exp. 2011

Couffinhal T, Silver M, Kearney M, Sullivan A, Witzenbichler B, Magner M, Annex B, Peters K, Isner JM. Impaired collateral vessel development associated with reduced expression of vascular endothelial growth factor in ApoE−/− mice. Circulation. 1999; 99(24):3188–3198. [PubMed: 10377084]

Coyle P, Heistad DD. Development of collaterals in the cerebral circulation. Blood Vessels. 1991; 28(1–3):183–189. [PubMed: 2001469]

Coyle P, Jokelainen PT. Dorsal cerebral arterial collaterals of the rat. Anat Rec. 1982; 203(3):397–404. [PubMed: 7137595]

Crisostomo EA, Bjorlin LC, Randolph RD, Himango WA. Development and disappearance of anterior cerebral artery collateral flow detected by transcranial Doppler sonography in a stroke patient. J Ultrasound Med. 1993; 12(7):419–422. [PubMed: 8355337]

Cuccione E, Padovano G, Versace A, Ferrarese C, Beretta S. Cerebral collateral circulation in experimental ischemic stroke. Exp Transl Stroke Med. 2016; 8:2. [PubMed: 26933488]

Deacon RM. Measuring the strength of mice. J Vis Exp. 2013; (76)

Defazio RA, Levy S, Morales CL, Levy RV, Dave KR, Lin HW, Abaffy T, Watson BD, Perez-Pinzon MA, Ohanna V. A protocol for characterizing the impact of collateral flow after distal middle cerebral artery occlusion. Transl Stroke Res. 2011; 2(1):112–127. [PubMed: 21593993]

Defazio RA, Zhao W, Deng X, Obenaus A, Ginsberg MD. Albumin therapy enhances collateral perfusion after laser-induced middle cerebral artery branch occlusion: a laser speckle contrast flow study. J Cereb Blood Flow Metab. 2012; 32(11):2012–2022. [PubMed: 22781334]

Drake CG, Peerless SJ, Ferguson GG. Hunterian proximal arterial occlusion for giant aneurysms of the carotid circulation. J Neurosurg. 1994; 81(5):656–665. [PubMed: 7931611]

Author Manuscript Author Manuscript Author Manuscript Author Manuscript

Flores-Rozas H, Kelman Z, Dean FB, Pan ZQ, Harper JW, Elledge SJ, O'Donnell M, Hurwitz J. Cdk-interacting protein 1 directly binds with proliferating cell nuclear antigen and inhibits DNA replication catalyzed by the DNA polymerase delta holoenzyme. Proc Natl Acad Sci U S A. 1994; 91(18):8655–8659. [PubMed: 7915843]

Fujie W, Kirino T, Tomukai N, Iwasawa T, Tamura A. Progressive shrinkage of the thalamus following middle cerebral artery occlusion in rats. Stroke. 1990; 21(10):1485–1488. [PubMed: 2219214]

Heil M, Ziegelhoeffer T, Pipp F, Kostin S, Martin S, Clauss M, Schaper W. Blood monocyte concentration is critical for enhancement of collateral artery growth. Am J Physiol Heart Circ Physiol. 2002; 283(6):H2411–2419. [PubMed: 12388258]

Heil M, Eitenmuller I, Schmitz-Rixen T, Schaper W. Arteriogenesis versus angiogenesis: similarities and differences. J Cell Mol Med. 2006; 10(1):45–55. [PubMed: 16563221]

Imura S, Miyake H, Izumi K, Tashiro S, Uehara H. Correlation of vascular endothelial cell proliferation with microvessel density and expression of vascular endothelial growth factor and basic fibroblast growth factor in hepatocellular carcinoma. J Med Invest. 2004; 51(3–4):202–209. [PubMed: 15460907]

Iwama T, Hashimoto N, Miyake H, Yonekawa Y. Direct revascularization to the anterior cerebral artery territory in patients with moyamoya disease: report of five cases. Neurosurgery. 1998; 42(5):1157–1161. discussion 1161-1152. [PubMed: 9588563]

Jones BJ, Roberts DJ. The quantiative measurement of motor incoordination in naive mice using an acelerating rotarod. J Pharm Pharmacol. 1968; 20(4):302–304. [PubMed: 4384609]

Jung S, Aliberti J, Graemmel P, Sunshine MJ, Kreutzberg GW, Sher A, Littman DR. Analysis of fractalkine receptor CX(3)CR1 function by targeted deletion and green fluorescent protein reporter gene insertion. Mol Cell Biol. 2000; 20(11):4106–4114. [PubMed: 10805752]

Jung S, Gilgen M, Slotboom J, El-Koussy M, Zubler C, Kiefer C, Luedi R, Mono ML, Heldner MR, Weck A, Mordasini P, Schroth G, Mattle HP, Arnold M, Gralla J, Fischer U. Factors that determine penumbral tissue loss in acute ischaemic stroke. Brain. 2013; 136(Pt 12):3554–3560. [PubMed: 24065722]

Kataoka K, Hayakawa T, Kuroda R, Yuguchi T, Yamada K. Cholinergic deafferentation after focal cerebral infarct in rats. Stroke. 1991; 22(10):1291–1296. [PubMed: 1926241]

Kennedy BK, Barbie DA, Classon M, Dyson N, Harlow E. Nuclear organization of DNA replication in primary mammalian cells. Genes Dev. 2000; 14(22):2855–2868. [PubMed: 11090133]

la Sala A, Pontecorvo L, Agresta A, Rosano G, Stabile E. Regulation of collateral blood vessel development by the innate and adaptive immune system. Trends Mol Med. 2012; 18(8):494–501. [PubMed: 22818027]

Li Y, Choi WJ, Qin W, Baran U, Habenicht LM, Wang RK. Optical coherence tomography based microangiography provides an ability to longitudinally image arteriogenesis in vivo. J Neurosci Methods. 2016; 274:164–171. [PubMed: 27751893]

Liebeskind DS, Jahan R, Nogueira RG, Zaidat OO, Saver JL, Investigators S. Impact of collaterals on successful revascularization in Solitaire FR with the intention for thrombectomy. Stroke. 2014; 45(7):2036–2040. [PubMed: 24876081]

Liebeskind DS. Collateral circulation. Stroke. 2003; 34(9):2279–2284. [PubMed: 12881609]

Liu ZS, Zhou LJ, Sun Y, Kuang XW, Wang W, Li C. Sufficient collateral blood supply from accessory middle cerebral artery in a patient with acute ischemic stroke. Interv Neuroradiol. 2015; 21(2): 215–217. [PubMed: 25943843]

Llovera G, Roth S, Plesnila N, Veltkamp R, Liesz A. Modeling stroke in mice: permanent coagulation of the distal middle cerebral artery. J Vis Exp. 2014:e51729. [PubMed: 25145316]

Lownie SP, Drake CG, Peerless SJ, Ferguson GG, Pelz DM. Clinical presentation and management of giant anterior communicating artery region aneurysms. J Neurosurg. 2000; 92(2):267–277. [PubMed: 10659014]

Lucitti JL, Mackey JK, Morrison JC, Haigh JJ, Adams RH, Faber JE. Formation of the collateral circulation is regulated by vascular endothelial growth factor-A and a disintegrin and metalloprotease family members 10 and 17. Circ Res. 2012; 111(12):1539–1550. [PubMed: 22965144]

Author Manuscript Author Manuscript Author Manuscript Author Manuscript

Meisner JK, Price RJ. Spatial and temporal coordination of bone marrow-derived cell activity during arteriogenesis: regulation of the endogenous response and therapeutic implications. Microcirculation. 2010; 17(8):583–599. [PubMed: 21044213]

Nishijima Y, Akamatsu Y, Weinstein PR, Liu J. Collaterals: implications in cerebral ischemic diseases and therapeutic interventions. Brain Res. 2015; 1623:18–29. [PubMed: 25770816]

Okyere B, Giridhar K, Hazy A, Chen M, Keimig D, Bielitz RC, Xie H, He JQ, Huckle WR, Theus MH. Endothelial-specific EphA4 negatively regulates native pial collateral formation and re-perfusion following hindlimb ischemia. PLoS One. 2016; 11(7):e0159930. [PubMed: 27467069]

Olton DS, Walker JA, Gage FH. Hippocampal connections and spatial discrimination. Brain Res. 1978; 139(2):295–308. [PubMed: 624061]

Raymond SB, Schaefer PW. Imaging brain collaterals: quantification, scoring, and potential significance. Top Magn Reson Imaging. 2017; 26(2):67–75. [PubMed: 28277461]

Schaffer CB, Friedman B, Nishimura N, Schroeder LF, Tsai PS, Ebner FF, Lyden PD, Kleinfeld D. Two-photon imaging of cortical surface microvessels reveals a robust redistribution in blood flow after vascular occlusion. PLoS Biol. 2006; 4(2):e22. [PubMed: 16379497]

Schaper W, Scholz D. Factors regulating arteriogenesis. Arterioscler Thromb Vasc Biol. 2003; 23(7): 1143–1151. [PubMed: 12676799]

Schierling W, Troidl K, Apfelbeck H, Troidl C, Kasprzak PM, Schaper W, Schmitz-Rixen T. Cerebral arteriogenesis is enhanced by pharmacological as well as fluid-shear-stress activation of the Trpv4 calcium channel. Eur J Vasc Endovasc Surg. 2011; 41(5):589–596. [PubMed: 21316269]

Scholz D, Ito W, Fleming I, Deindl E, Sauer A, Wiesnet M, Busse R, Schaper J, Schaper W. Ultrastructure and molecular histology of rabbit hind-limb collateral artery growth (arteriogenesis). Virchows Arch. 2000; 436(3):257–270. [PubMed: 10782885]

Shuaib A, Butcher K, Mohammad AA, Saqqur M, Liebeskind DS. Collateral blood vessels in acute ischaemic stroke: a potential therapeutic target. Lancet Neurol. 2011; 10(10):909–921. [PubMed: 21939900]

Squire LR, Ojemann JG, Miezin FM, Petersen SE, Videen TO, Raichle ME. Activation of the hippocampus in normal humans: a functional anatomical study of memory. Proc Natl Acad Sci U S A. 1992; 89(5):1837–1841. [PubMed: 1542680]

Squire LR. Memory and the hippocampus: a synthesis from findings with rats, monkeys, and humans. Psychol Rev. 1992; 99(2):195–231. [PubMed: 1594723]

Stabile E, Burnett MS, Watkins C, Kinnaird T, Bachis A, la Sala A, Miller JM, Shou M, Epstein SE, Fuchs S. Impaired arteriogenic response to acute hindlimb ischemia in CD4-knockout mice. Circulation. 2003; 108(2):205–210. [PubMed: 12821542]

Stabile E, Kinnaird T, la Sala A, Hanson SK, Watkins C, Campia U, Shou M, Zbinden S, Fuchs S, Kornfeld H, Epstein SE, Burnett MS. CD8+ T lymphocytes regulate the arteriogenic response to ischemia by infiltrating the site of collateral vessel development and recruiting CD4+ mononuclear cells through the expression of interleukin-16. Circulation. 2006; 113(1):118–124. [PubMed: 16380545]

Takahashi M, Miyauchi T, Kowada M. Computed tomography of Moyamoya disease: demonstration of occluded arteries and collateral vessels as important diagnostic signs. Radiology. 1980; 134(3): 671–676. [PubMed: 7355216]

Takahashi M. Magnification angiography in moyamoya disease: new observations on collateral vessels. Radiology. 1980; 136(2):379–386. [PubMed: 7403514]

Theus MH, Wei L, Cui L, Francis K, Hu X, Keogh C, Yu SP. In vitro hypoxic preconditioning of embryonic stem cells as a strategy of promoting cell survival and functional benefits after transplantation into the ischemic rat brain. Exp Neurol. 2008; 210(2):656–670. [PubMed: 18279854]

Toriumi H, Tatarishvili J, Tomita M, Tomita Y, Unekawa M, Suzuki N. Dually supplied T-junctions in arteriolo-arteriolar anastomosis in mice: key to local hemodynamic homeostasis in normal and ischemic states? Stroke. 2009; 40(10):3378–3383. [PubMed: 19661466]

Troidl C, Jung G, Troidl K, Hoffmann J, Mollmann H, Nef H, Schaper W, Hamm CW, Schmitz-Rixen T. The temporal and spatial distribution of macrophage subpopulations during arteriogenesis. Curr Vasc Pharmacol. 2013; 11(1):5–12. [PubMed: 23391417]

Author Manuscript Author Manuscript Author Manuscript Author Manuscript

van Royen N, Piek JJ, Buschmann I, Hoefer I, Voskuil M, Schaper W. Stimulation of arteriogenesis; a new concept for the treatment of arterial occlusive disease. Cardiovasc Res. 2001; 49(3):543–553. [PubMed: 11166267]

van Seeters T, Biessels GJ, Kappelle LJ, van der Graaf Y, Velthuis BK, i Dutch acute stroke study. Determinants of leptomeningeal collateral flow in stroke patients with a middle cerebral artery occlusion. Neuroradiology. 2016; 58(10):969–977. [PubMed: 27438804]

Winship IR. Cerebral collaterals and collateral therapeutics for acute ischemic stroke. Microcirculation. 2015; 22(3):228–236. [PubMed: 25351102]

Wolf C, Cai WJ, Vosschulte R, Koltai S, Mousavipour D, Scholz D, Afsah-Hedjri A, Schaper W, Schaper J. Vascular remodeling and altered protein expression during growth of coronary collateral arteries. J Mol Cell Cardiol. 1998; 30(11):2291–2305. [PubMed: 9925366]

Yamada I, Murata Y, Umehara I, Suzuki S, Matsushima Y. SPECT and MRI evaluations of the posterior circulation in moyamoya disease. J Nucl Med. 1996; 37(10):1613–1617. [PubMed: 8862293]

Zhang H, Prabhakar P, Sealock R, Faber JE. Wide genetic variation in the native pial collateral circulation is a major determinant of variation in severity of stroke. J Cereb Blood Flow Metab. 2010; 30(5):923–934. [PubMed: 20125182]

Zhang S, Zhang X, Yan S, Lai Y, Han Q, Sun J, Zhang M, Parsons MW, Wang S, Lou M. The velocity of collateral filling predicts recanalization in acute ischemic stroke after intravenous thrombolysis. Sci Rep. 2016; 6:27880. [PubMed: 27296511]

Author Manuscript Author Manuscript Author Manuscript Author Manuscript

HIGHLIGHTS

- Vessel painting highlights collateral remodeling induced by pMCAO.
- Collateral diameter peaks at 4 days post-pMCAO in CD1 mice.
- Vessel painting can be combined with immunofluorescence labeling.

Author Manuscript Author Manuscript Author Manuscript Author Manuscript

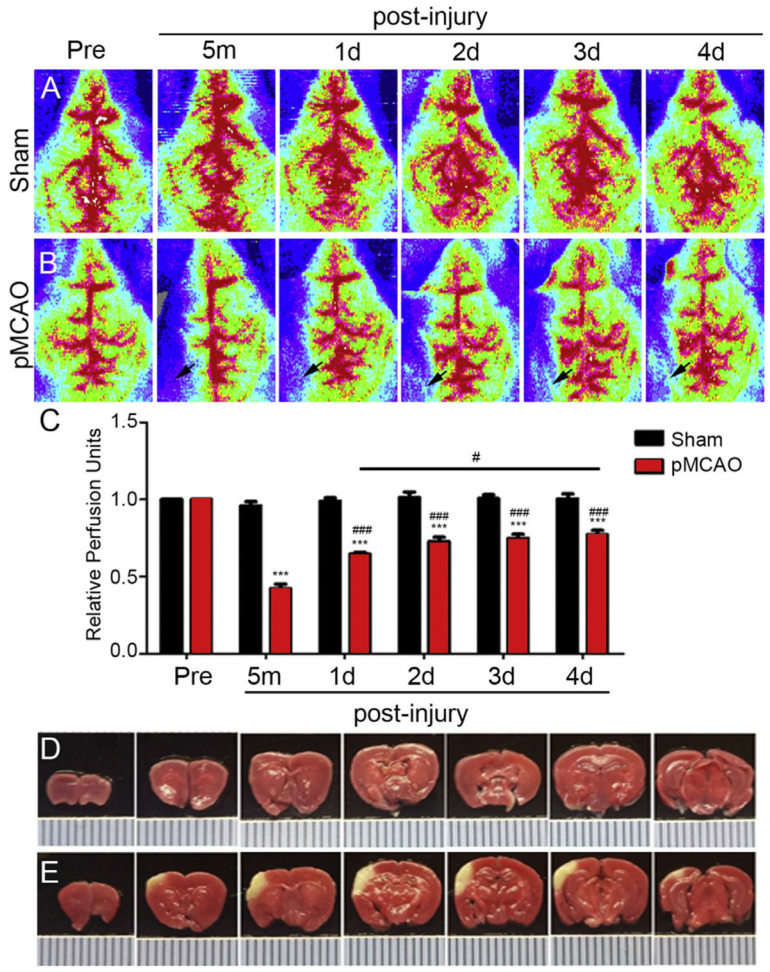

Fig. 1.

Cerebral Blood Flow (CBF) following pMCAO. Transverse Laser Doppler image analysis of CBF at 1–4 day pre- and post-sham (A) and – pMCAO (B) in adult CD1 mice. Arrow indicates region of reduced CBF and area of reperfusion in the ipsilateral hemisphere after pMCAO. (C) Quantitative analysis shows a significant decrease in ipsilateral CBF at 5 min post-pMCAO relative to pre-injury. Partial restoration of ipsilateral CBF occurs at 1–4 days compared to 5 min post-pMCAO. There was also a significant restoration of CBF between 1d and 4d post-pMCAO. No differences in CBF were observed in sham-injury mice. (D) Triphenyl tetrazolium chloride (TTC)-stained mouse coronal brain slices after 1 day sham injury compared to pMCAO (C). Area of infarct appears white compared to healthy red-stained tissue. Hash marks = 1 mm in D and E.***$P < 0.001$ compared to sham; #$P < 0.05$ compared to 1d pMCAO; ###$P < 0.001$ compared to 5 min post-pMCAO (n = 5–7 mice per group). Data represented as mean ± SEM.

Author Manuscript Author Manuscript Author Manuscript Author Manuscript

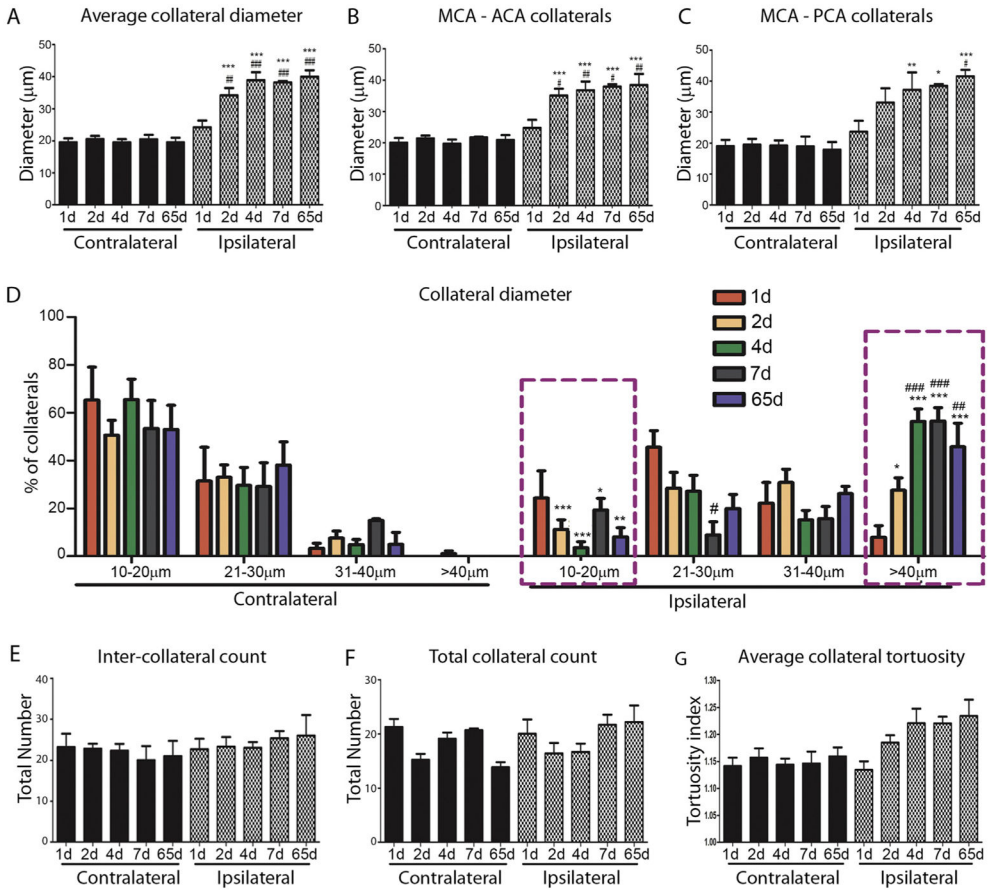

Fig. 2.

Analysis of pial collateral remodeling after pMCAO. (A) Average collateral diameter (μm) in the contralateral and ipsilateral hemispheres at 1, 2, 4, 7 and 65 days post-pMCAO. Ipsilateral collateral diameter is significantly increased following pMCAO compared to contralateral at all time points except at 1 day (***P < 0.001). Additionally, there was a significant increase in ipsilateral collateral diameter at 2, 4, 7 and 65 days compared to 1 day post-pMCAO (##P < 0.01; ###P < 0.001). These findings were similar when analyzing MCA-ACA (B) and MCA-PCA (C) collaterals. (D) Percentage of collaterals measuring 10–20 μm, 21–30 μm, 31–40 μm, >40 μm on the contra- and ipsilateral hemispheres. The largest change was observed in vessels >40 μm at 2–65 days post-pMCAO. Less than 1% of contralateral collaterals measured >40 μm, however, a significant increase was seen in ipsilateral vessels at 2 days (~30%) and 4, 7 and 65 days (~60%) compared to 1 day (~10%). (E) The numbers of inter-collaterals (MCA-ACA and MCA-PCA) and (F) total number of collaterals was unchanged following pMCAO. (G) A trend towards increased tortuosity of ipsilateral collaterals was also seen at 2–65 days post-pMCAO compared to contralateral. *p < 0.05; **p < 0.01; ***p < 0.001 compared to contralateral at each individual time point; #p < 0.05; ##p < 0.01; ###p < 0.001 compared to 1 day ipsilateral post-pMCAO (n = 5–9 mice/group). Data represented as mean ± SEM.

Author Manuscript Author Manuscript Author Manuscript Author Manuscript

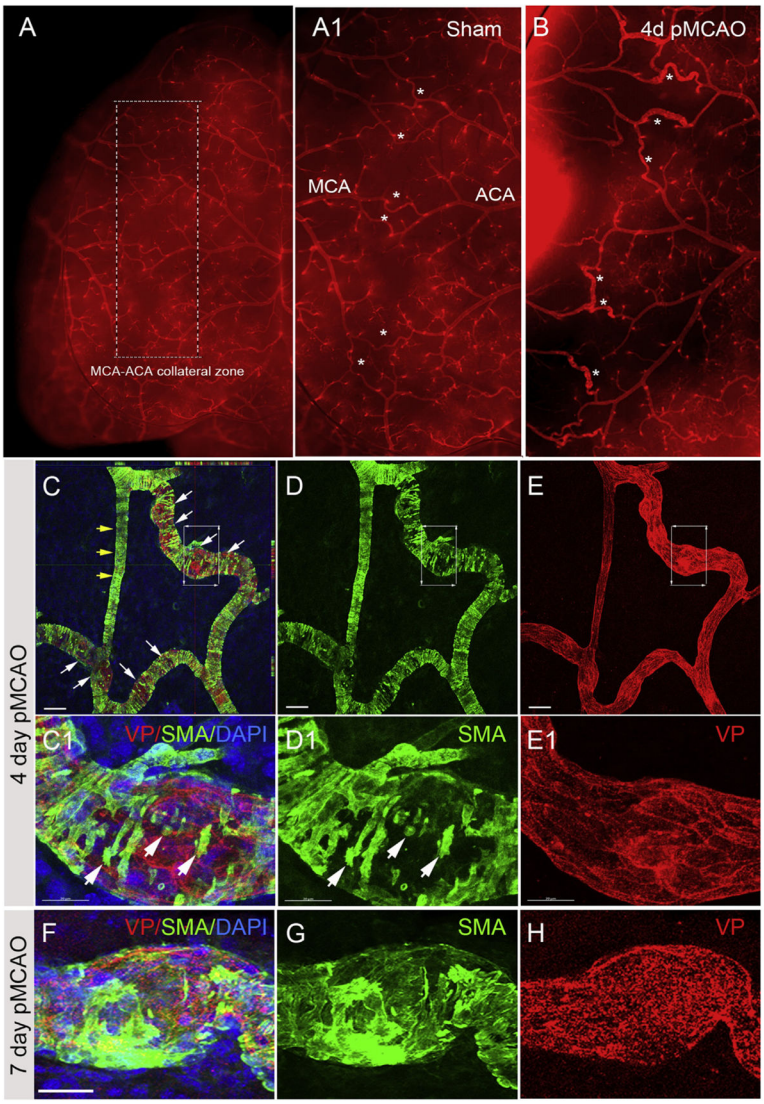

Fig. 3.

Histological evaluation of pial collateral remodeling. (A) Identification of pial collaterals using vessel painting (VP, red). Arrows indicate MCA-ACA collaterals at 1 day post-sham in the ipsilateral hemisphere compared to 1d (B), 2d (C) and 4d (D) post-pMCAO. (E–H) Confocal image analysis of VP co-labeled with anti-SMA showing dynamic changes in SMA expression at 1 day (E) and 4 day (F) post-pMCAO. (G) Representative high magnification images of a stable collateral vessel in the contralateral region compared to a remodeling collateral in the ipsilateral hemisphere (H) at 4 days post-pMCAO. Scale bar = 200 μm in E and F; Scale bar = 20 μm in E1–E3, F1–F3 and G–H. (For interpretation of the references to colour in this figure legend, the reader is referred to the web version of this article.)

Author Manuscript Author Manuscript Author Manuscript Author Manuscript

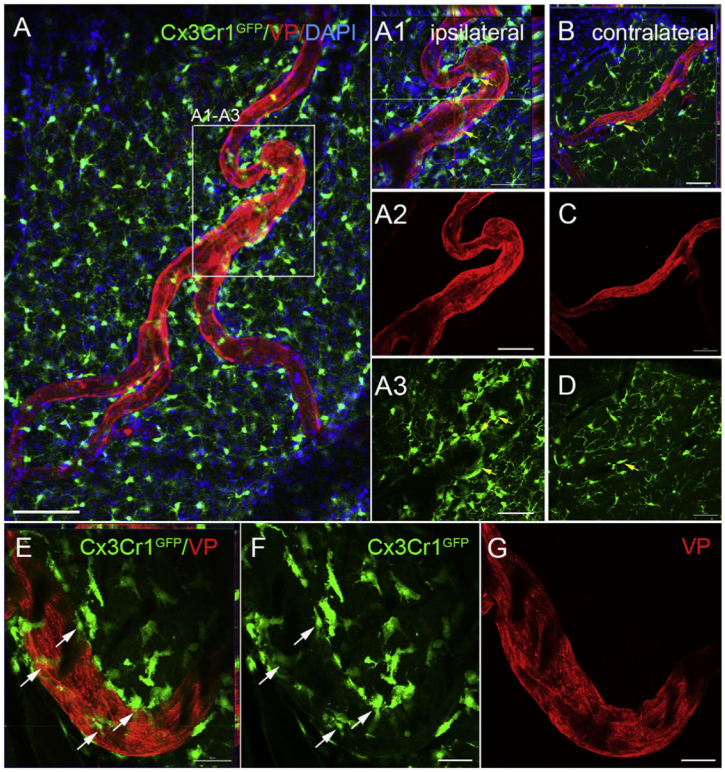

Fig. 4.

Analysis of collateral remodeling in vessel painted Cx3Cr1^{GFP} mice after pMCAO. (A) Representative confocal microscopy showing Cx3Cr1^{GFP}-expressing immune-derived cells (green) co-labeled with vessel painting (VP; red) and 4′,6-diamidino-2-phenylindole (DAPI; blue) (A1–A3) in the ipsilateral hemisphere of whole mount cortical tissue at 4 days post-pMCAO. Numerous GFP-positive cells were attached to and surrounding the collaterals undergoing remodeling. (B–D) Few to no GFP-positive cells are present on contralateral collaterals. GFP-positive cells are also observed in the underlying tissue, likely parenchymal microglia. (E–G) High magnification confocal image demonstrating extensive recruitment of GFP-positive cells to the remodeling collateral vessels in the ipsilateral hemisphere. Scale bar = 200 μm in A; 50 μm in A1–A3, E–G; 20μm in B–D. (For interpretation of the references to colour in this figure legend, the reader is referred to the web version of this article.)

Author Manuscript Author Manuscript Author Manuscript Author Manuscript

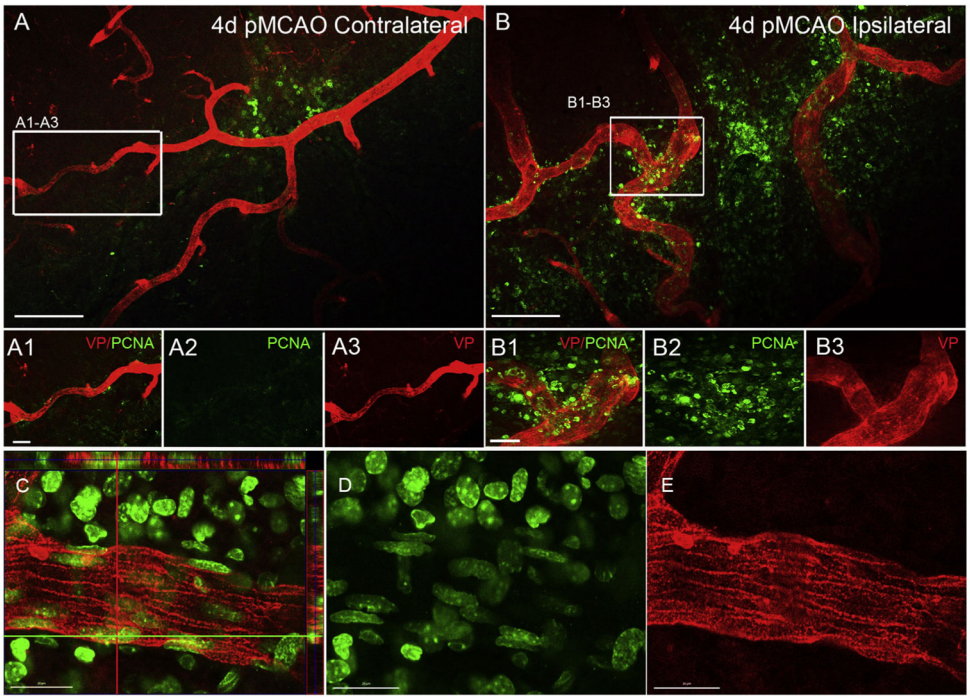

Fig. 5.

Analysis of cellular proliferation in the pial collateral niche after pMCAO. (A and B) PCNA labeling of proliferating cells in collateral zone of whole mount cortical tissue at 4 days post-pMCAO. Extensive PCNA labeling is seen in the underlying injured cortex, remodeling collaterals and large veins. PCNA expression (green) is present around remodeling collateral vessels in the ipsilateral side (B1–B2) but not on vessels in the contralateral hemisphere (A1–A3). Scale bar = 200 μm in A and B; 20 μm in A1–A3 and B1–B3. (C–E) Representative high magnification images of a growing ipsilateral collateral at 4d post-pMCAO showing PCNA expression in the vessel painted wall of the collateral. Scale bar = 20 μm. (For interpretation of the references to colour in this figure legend, the reader is referred to the web version of this article.)

Author Manuscript Author Manuscript Author Manuscript Author Manuscript

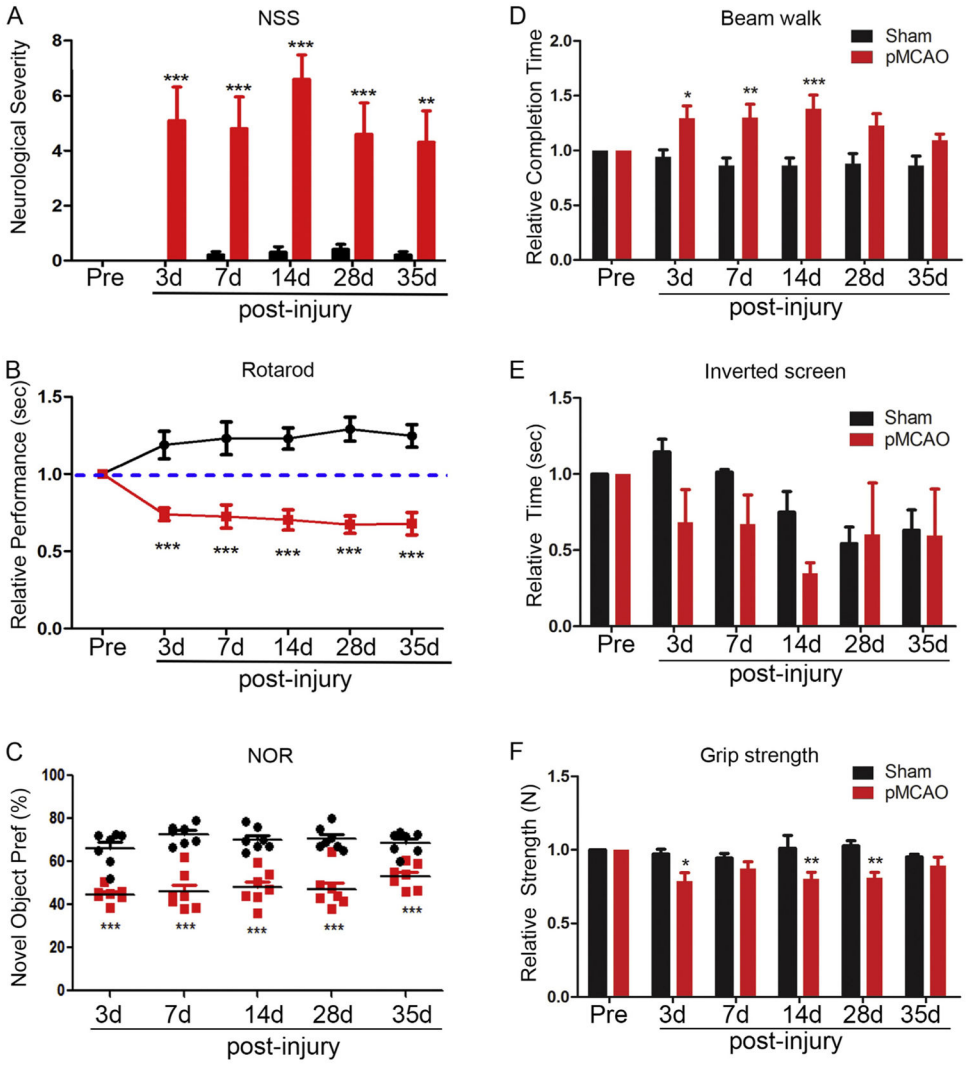

Fig. 6.

Comprehensive analysis of behavioral deficits after pMCAO. Comprehensive sensorimotor and cognitive behavioral tasks were quantitatively assessed at 3–35 days post-sham and –pMCAO injury. (A) Quantitative assessment of Neurological Severity Scoring (NSS) post-injury showed sham-injured animals have significantly lower severity score compared to pMCAO mice. (B) Rotarod assessment demonstrated focal ischemia causes significant motor impairment that is sustained from 3 to 35 days after injury. (C) Novel object recognition was also significantly reduced in pMCAO mice at all the time points tested post-injury. (D) Completion time on the beam walk was also significantly increased following pMCAO, indicating mice required more time to traverse a narrow beam owing to functional impairments. (E) Inverted screen assessment shows no consistent performance difference in sham or pMCAO-injured mice. (F) Assessment of relative strength in injured mice using grip assessment. Analyses indicate relative deficits in strength at each time point and significant difference at 3d, 14d and 28d post-pMCAO compared to sham injury. *P < 0.05; **P < 0.01 and ***P < 0.001 compared to sham controls.